

## The phase transition diagram of the $\Phi_3^6$ theory

**Marcia G. Amaral and Ronald C. Shellard**

*Departamento de Física, Pontifícia Universidade Católica do Rio de Janeiro, Caixa Postal 381171, Rio de Janeiro, 22453, RJ, Brasil*

Received on September 9, 1988

**Abstract** We study the structure of tricritical points in continuum theories using as a prototype the  $\Phi_3^6$  theory in three dimensions. We map the phase transition surfaces, localizing the tricritical line. We define the theory on a lattice and use the Monte Carlo method to perform the numerical simulation.

### 1. Introduction

There are many models which exhibit phase transitions of second order which change to first order at tricritical points, such as the Abelian Higgs model both at  $d = 4$ <sup>1,3</sup> and  $d = 3$ <sup>4</sup> and the SU(2) Higgs model with scalar fields<sup>2</sup>. The main problem with these models is that we still do not know how the order of the transition lines in these models will be affected by the use of larger and larger lattices.

In this paper we study the phase diagram of the  $\eta\Phi_3^6$  theory using the Monte Carlo numerical simulation method. We were motivated to approach this system, in order to understand the structure of tricritical points, which we have encountered in the study of the Abelian Higgs model at  $d = 4$ <sup>3</sup> and  $d = 3$ <sup>4</sup>. The  $\eta\Phi_3^6$  is the simplest system, with continuous variables, which exhibits this phenomenon,

---

Work partially supported by FINEP, CAPES and CNPq.

### *The phase transition diagram of the $\Phi_3^6$ theory*

and it allows us to study with care the dependence of the order of the phase transition lines and the position of the tricritical points with the lattice size. The large  $N$  limit of the  $\Phi_3^6$  theory was studied recently<sup>5</sup> and it has been observed that  $N \simeq 30$  is the lower bound for the occurrence of the Bardeen, Moshe and Bander (BMB) phenomena<sup>6</sup>. In the phase diagram for these large values of  $N$ , the second order transition line ends on the first order line such that the first order line continuous into the  $O(N)$ -symmetric phase, while for values of  $N < 30$  the second order line goes over into the first order line leading to a tricritical point.

In this paper we study the phase diagram of this theory in the space of parameters  $\mu, \nu$  and  $a'$ , to be defined below. We establish the contour for the region of second order and first order transition in the phase transition surfaces. We subject the system to an small external magnetic current in order to expose the phase transition line. On a second order line, the external field drives the magnetization slightly out of the discontinuity, forcing it to take a finite value which can be identified as the expectation value of the order parameter at the transition. This method is very effective, allowing the simulation to be done with a not so large a number of Monte Carlo steps. We study this model using lattices that range from 5 sites to 15 sites in order to study the dependence of the order of the phase transition lines with the lattice volume.

## **2. The $\Phi_3^6$ theory**

We investigate in this work the theory defined in the continuum by the Euclidean Lagrangian

$$L_e = +\frac{1}{2}(\partial_\mu \phi)^2 + V(\Phi) + j\Phi \quad (1)$$

where the field  $\Phi$  is real and

$$V(\Phi) = \frac{1}{2}m^2\Phi^2 + \frac{\lambda}{4}\Phi^4 + \frac{\eta}{6}\Phi^6 \quad (2)$$

It is convenient to rewrite this potential in the form

$$V(\Phi) = \frac{1}{6}\eta\left(\Phi^2 - \frac{\sigma}{\eta}\right)^2\left(\Phi^2 - \frac{\omega}{\eta}\right) \quad (3)$$

such that its structure is more transparent. The relations between the parameters of both potentials are given by

$$m^2 = \frac{1}{3\eta}\sigma(2\omega + \sigma) \quad (4)$$

When  $\omega \leq 0$ , the theory is uninteresting, since the potential has a simple structure, having a single minimum at  $Q = 0$  and growing monotonically with  $Q$ . We will consider in this study the case where  $\sigma > 0$ , only.

We rescale the field  $\phi$ , making it dimensionless through

$$\theta^2 \equiv \frac{\eta\Phi^2}{\sigma} \quad (6)$$

and defining the dimensionless parameter

$$\nu \equiv \omega/\sigma \quad (7)$$

such that the potential

$$V(\theta) = \frac{\sigma^3}{6\eta^2}(\theta^2 - 1)^2(\theta^2 - \nu) \quad (8)$$

has the behavior depicted in the fig. 1, as  $\nu$  varies. When  $\nu < -1$  the potential has a double minimum at  $\theta^2 = 1$  and we expect the phase transition to be analogous to that of the  $\chi Q^4$  theory (fig.1a); when  $-1 < \nu < 1$ , the potential has a triple minimum, at  $\theta^2 = 1$  and  $\theta = 0$ . There, one may expect a first order phase transition for values of  $\nu$  near zero, where the minima of the potential are degenerate. (Fig. 1b and 1c). When  $\nu > 1$  the points  $\theta^2 = 1$ , are now maxima and the minima occur at  $\theta = 0$  and  $\theta^2 = (1 + \nu)/2$ . The minima at  $\theta \neq 0$  will be lower than that at  $\theta = 0$ , for values of  $\nu > \nu_c = 4.236\dots$ , therefore we expect a first order transition for  $\nu \simeq \nu_c$ .

The phase transition diagram of the  $\Phi_3^6$  theory

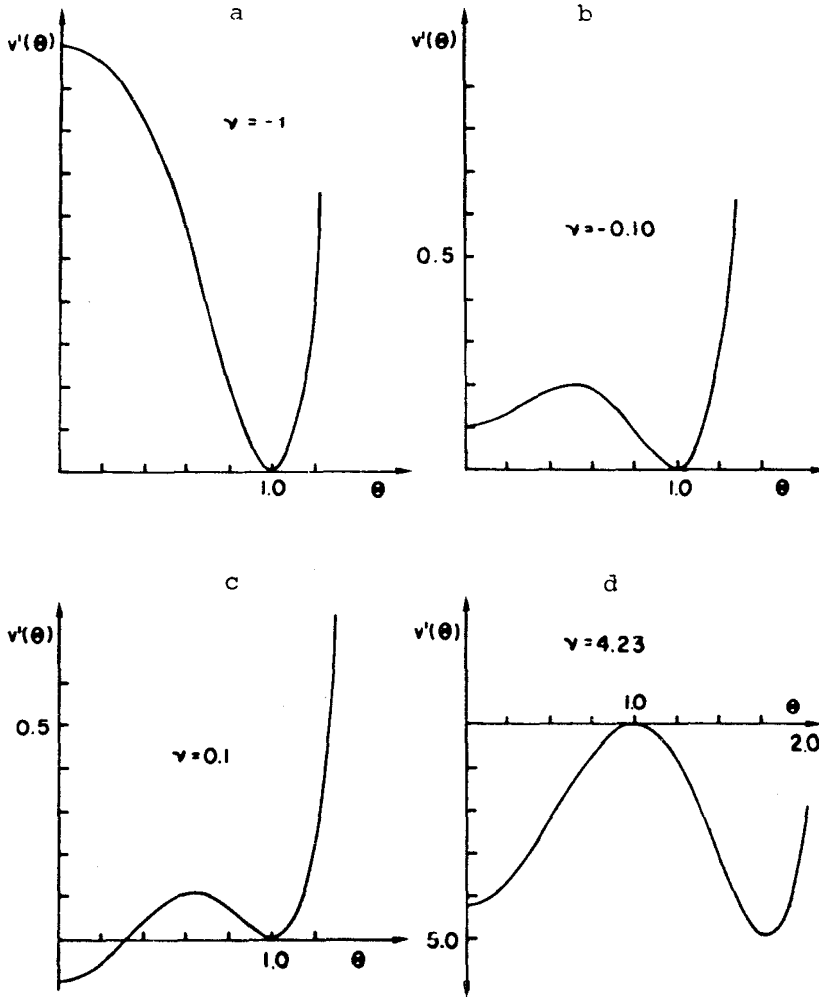


Fig.1 - Behaviour of the potential  $V(\theta) = (O^2 - 1)^2 (\theta^2 - \nu) / 6$  for different values of  $\nu$ .

The lattice version of this theory is written in terms of the action

$$S(\theta) = \beta \sum_n \left\{ -\chi \sum_{\mu} \theta(\vec{n} + \hat{\mu}) \theta(\vec{n}) + 3\chi \theta^2 + (\theta^2(\vec{n}) - 1)^2 (\theta^2(\vec{n}) - \nu) \right\} + J \sum_n \theta(\vec{n}) \quad (9)$$

where we have replaced the continuum derivative by

$$\partial_\mu \theta \rightarrow \frac{(\vec{n} + \hat{\mu}) - \theta(\vec{n})}{a} \quad (10)$$

$a$  is the lattice spacing,

$$\chi = \eta/a^2 a^2 \quad (11)$$

and

$$\beta = a^3 a^3 / \eta^2 \quad (12)$$

It is more convenient to present the numerical results in terms of the parameters  $\nu, \eta$  and  $a' = (\chi^{-1/2})$ . In the limit  $\eta \rightarrow 0$ , the theory collapses into the  $\lambda\Phi_3^4$  model, which is a non trivial theory. In this limit,  $a \rightarrow_{\eta \rightarrow 0} 4 \frac{\eta m^2}{\lambda}$ , so that the inverse temperature  $\beta$  is proportional to  $\eta$ , however the products  $\beta\chi$  and  $\beta\nu$  remain finite and this point corresponds to  $\nu \rightarrow \infty$  on then  $\eta = a' = 0$  axis.

### 3. Numerical simulation of the phase diagram

We performed the numerical simulation of the  $\eta\Phi_3^6$  model using the Monte Carlo method with the Metropolis algorithm. To generate a new trial field at each site, we chose a random value in a given interval. We controled the width of the interval by plotting the accepted fields distribution and allowing a safety margin on each side of the distribution. We adjusted the safety margin by having an acceptance rate for new fields at each trial around 0.5.

We searched for the transition line by running first hysteresis loops on coarse grained lattices with  $5^3$  points. After that, we repeated the hysteresis loop on large lattices of  $15^3$  points, to localize the transition line with higher resolution, keeping all parameters equal. Actually, the coarse grained approximation to the transition line gives a good resolution line.

When doing a complete Monte Carlo simulation for a set of parameters, we typically run through 10000 configurations, discarding the first 2000 allowing for thermalization. We used only every hundredth configuration, thus avoiding correlations between them, to compute averages. In order to improve the efficiency of our code, we did between 5 and 10 trials to change the value of the field at each site, before moving to the next site.

*The phase transition diagram of the  $\Phi_3^6$  theory*

We use a small external magnetic field to drive the transition. The magnetic field will push the expectation value of the order parameter towards a finite value, when the system is in the broken symmetry phase across a second order phase transition. The diagram of  $\mathbf{j}$  versus  $\langle 0 \rangle$  which is used to compute the effective potential in the region mentioned, has a flat piece at  $\mathbf{j} = 0$ , and then a piece which increases sharply starting at 0, for  $j \gtrsim 0$ , so that the small value of  $j$  drives  $\langle 0 \rangle$  towards 0<sup>7</sup>. We checked that the appropriate value for  $j$  was used in each case, by computing in a coarse grained lattice the  $\mathbf{j}$  versus  $\langle 0 \rangle$  diagram. However, this trick is not of much use in the regions across a first order phase transition, for there the flat piece of the  $\mathbf{j} < 0 \rangle$  diagram occurs at finite values of  $j$ . Nevertheless, this  $j < 0 \rangle$  diagram is of help in identifying the nature of a phase transition.

There is a phase transition surface in the  $\eta\nu a'$  space, which follows roughly the  $\nu a'$  plane at the  $\nu = 0$  axis. The phase transition lines in the  $\eta\nu$  plane for different values of  $a'$  are shown in the fig. 2. There the first order transition is indicated by a full line, while the second order piece is indicated by the broken line. For small values of  $a'$  and large values of  $\eta$  the transition line seems to bent in the direction of large and negative values of  $\nu$ . As we are mainly interested in studying the structure of tricritical points of this model we have not shown in this figure that part of the parameter space. The section of the surface on the  $a'\nu$  plane at  $\eta = 0.001$ , described in the previous figure, is shown in figure 3. We have computed the transition line at a value of  $\eta$  small but not zero, for then one has  $\beta \rightarrow \infty$ ,  $\beta\chi = 4m^2 a/\lambda$  and  $\beta\nu = 36m^2 a^3/X$ . However  $a'$  and  $\nu$  can be kept finite, provided that  $\lambda^2$  goes to zero at the same rate as  $\eta$ . But then, the effective temperature of the system,  $(\beta\chi)^{-1}$ , goes to zero. The transition stays at a value of  $\nu$  close to zero as  $a'$  grows large, implying that the value of  $m^2$  is also very small. There is a piece of this transition line which is first order for a certain range of  $a'$ . The field distribution of the configurations, at  $q = 0.0001$ ,  $a' = 2.0$  and  $\nu$  around a first order transition point is shown in fig. 4. This field distribution is computed by summing all field configurations used to compute the Monte Carlo averages, counting their contribution to each bin of specified length, and then normalizing the integral of the distribution to 1. In this figure we may observe that the field

distribution jumps from a strongly peaked distribution near  $\langle \theta \rangle \simeq 1$ , to a distribution peaked near  $\nu \simeq 0.120$ . The strongly peaked distribution are a reflex of the small energy stored in the kinetic part of the Lagrangean.

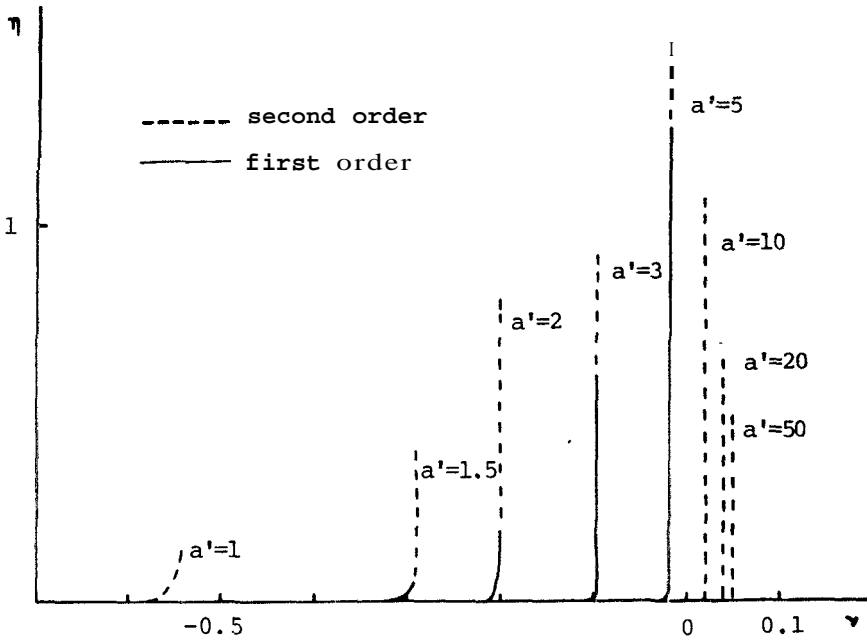


Fig.2 - Phase transition line in the  $\eta\nu$  plane, for different values of  $a'$ . The solid lines correspond to first order transitions, while the broken ones are second order.

The phase transition points are localized through the use of hysteresis loops. We show in fig. 5 an example of hysteresis loop in  $\nu$  taken at  $a' = 3.0$ , for different values of  $\eta$ . In this diagram the differences between first and second order transitions appear clearly. While figs.5a and 5b, for  $\eta = 0.8$  and  $0.6$  show no gap in the loop, 5c and 5d, corresponding to  $\eta = 0.5$  and  $0.3$  show a gap which widens as  $\eta$  is lowered, characteristic of first order transitions. The tricritical point at  $a' = 3.0$  is located between  $\eta = 0.5$  and  $0.6$ . The arrows in the diagram indicate the phase transition point, taken to be the middle point between the points where

The phase transition diagram of the  $\Phi_3^6$  theory

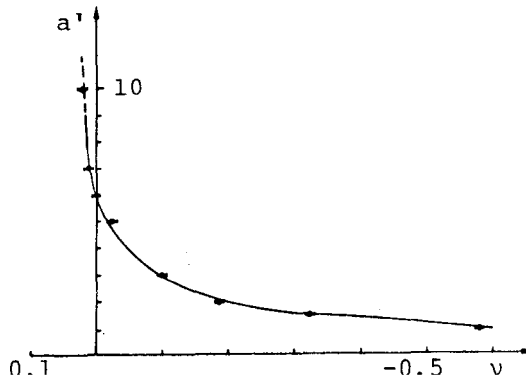


Fig.3 - The phase diagram at  $\eta = 0.001$  in the  $a' \nu$  plane. The solid line is a first order transition while the dashed line corresponds to a second order line.

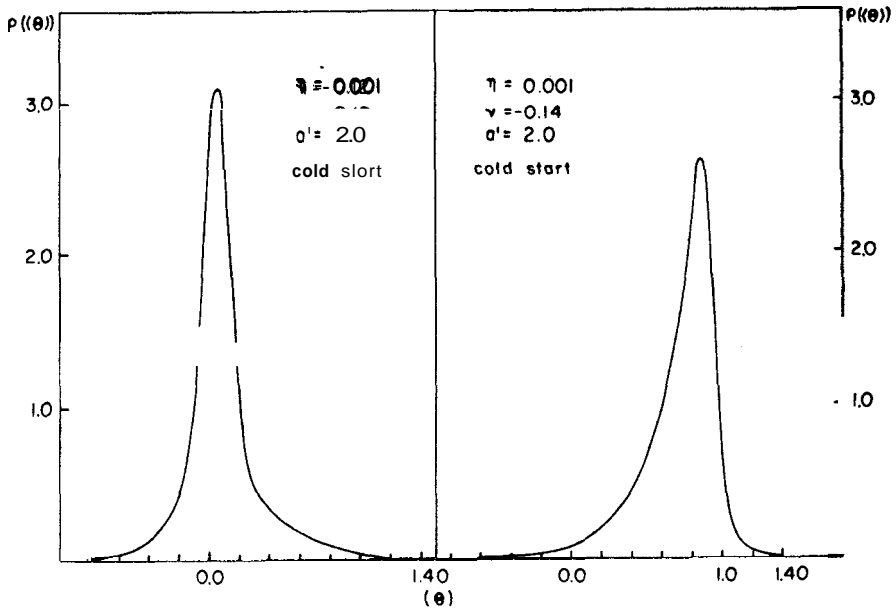


Fig.4 - The field distribution at two values of  $\nu$  at  $a' = 2.0$ ,  $\eta = 0.001$ , on different sides of the phase transition surface.

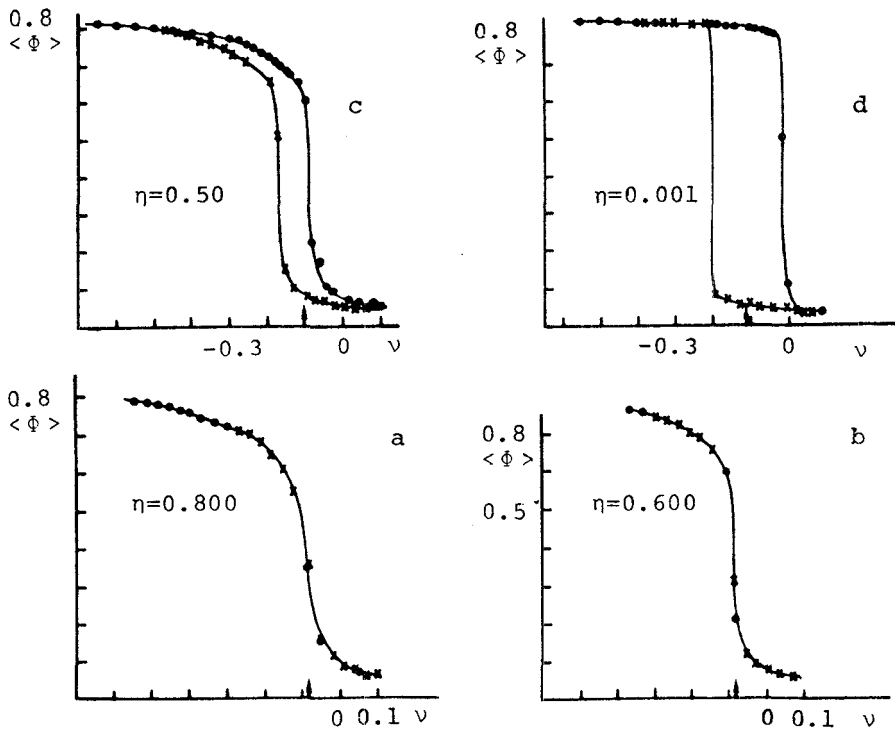


Fig.5 - Hysteresis loop in the  $\nu$  parameter at  $a' = 3.0$ . Diagrams a) and b) show a second order transition, while c) and d) are first order loops. The arrows indicate the position of the phase transition.

the hysteresis loop has maximum derivative. The nature of the phase transition is checked through the Monte Carlo evolution of the system, starting from two different initial configurations, either cold, where **all** fields are ordered and take the **value** where the classical potential is a minimum, or hot, where the fields take random values. An example of this Monte Carlo time evolution is shown in **fig. 6**, for  $a' = 3.0$  and for the values of  $\eta$  shown in **fig. 5**. There, for  $\eta \geq 0.6$ , the evolution shows the characteristics behaviour of second order phase transitions, while for  $\eta \leq 0.6$  the **existence** of two metastable configurations, indicated by a gap opening is typical of first order transitions.

The phase transition diagram of the  $\Phi_3^6$  theory

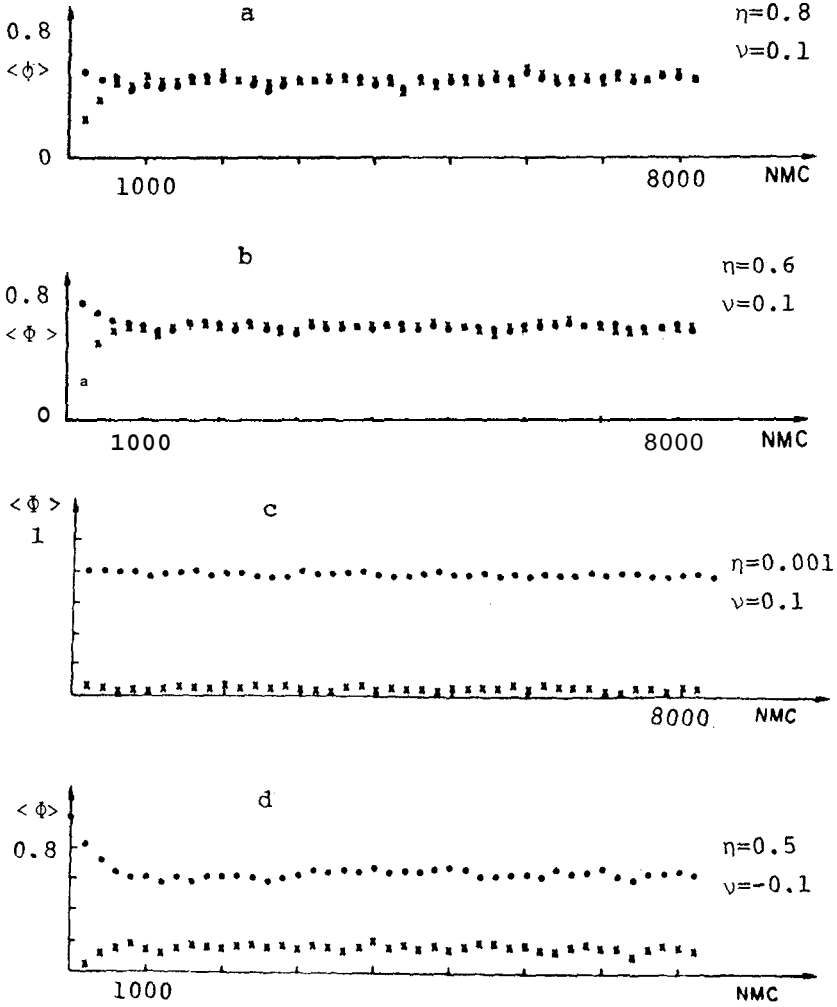


Fig.6 - Monte Carlo time evolution starting from hot and cold initial configurations. Diagrams a) and b) show second order behaviour, while c) and d) show a gap, typical of first order.

We may summarize the tricritical line in the surface of phase transitions around  $\nu \simeq 0$ , in fig.7, by plotting the contour of the first order region projected on the  $a'$  plane. The contour of the first order region shows a peak at  $a' = 6.7 \pm 0.1$ , with a maximum value  $\eta = 2.22 \pm 0.04$ . We have checked the position of this peak in  $a$  and  $\tau$ , running simulations in lattice  $\zeta$  with  $5^3$ ,  $10^3$  and  $15^3$  sites. The position of the peak and its value in are quite insensitive to the size of the lattice.

We summarize in fig. 8 the other phase transition surface which is roughly parallel to the one described above, around  $\eta = \nu_c$  ( $= 4.236\dots$ ).

#### 4. Summary

We have investigated the phase structure of the  $\eta\phi_3^6$  in 3 dimensions using a Monte Carlo simulation on lattices of size  $15^3$ . We intended to map the tricritical line on the phase transition surfaces. We found that the phase transition surfaces are quite insensitive to the size of the lattice, allowing us to use data generated by configurations of size  $5^3$ , and to check some of this simulation data by running configurations with  $15^3$  sites. This theory is particularly proper to emulate the structure of systems where a tricritical transition occurs.

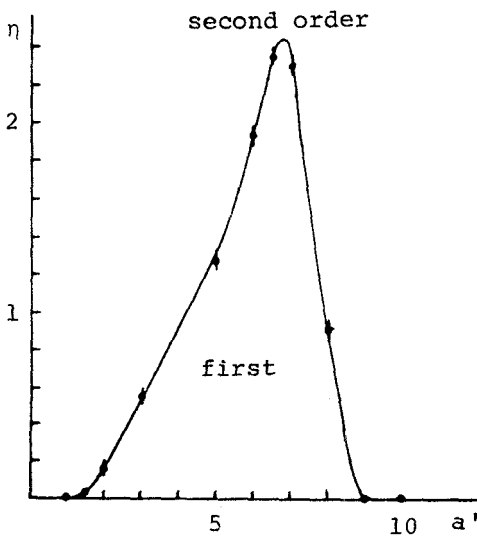


Fig.7 - Line of tricritical points on the phase transition surface.

The phase transition diagram of the  $\Phi_3^6$  theory

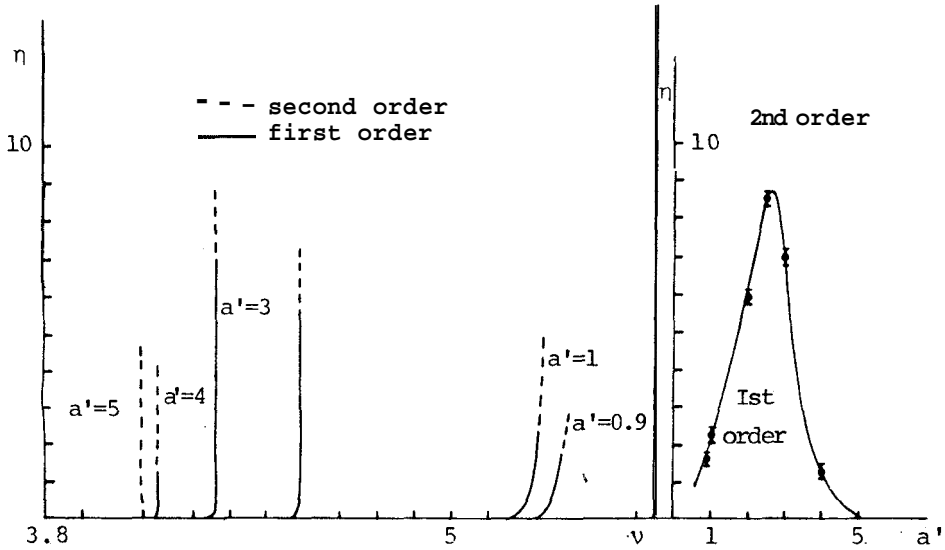


Fig.8 - Phase transition lines in the  $\eta$  plane, for different values of  $a'$ , for the surface around  $\nu_c = 4.236\dots$

## References

1. Y. Munehisa, Phys. Rev. D30, 1310 (1984). G. Koutsoumbas, Phys. Lett. **140B**, 379 (1984). V.P. Gerdt, A.S. Ilchev and V.K. Mitrjushkin, Yad. Fiz. 40, 1097 (1984). D. Espriu and J.F. Wheeler, Nucl. Phys. **B258**, 101 (1985). K. Jansen, J. Jersak, C.B. Lang, T. Neuhaus and G. Vones, Phys. Lett. **155B**, 268 (1985); Nucl. Phys. **B265** [FS15], 129 (1986).
2. J. Jersak, C.B. Lang, T. Neuhaus and G. Vones, Phys. Rev. **D32**, 2761 (1985). V. Gerdt, A.S. Alchev, V.K. Mitrjushkin, I.K. Sobolev and A.M. Zadorozhny, Nucl. Phys. B265 [FS15], 145 (1986). J. Jersak in Lattice Gauge Theory, A Challenge in Large Scale Computing, B. Bunk, K.H. Mütter and K. Schilling eds., Plenum Press, NY and London, (1986).
3. M.G. Amaral, M.E. Pol and R.C. Shellard, J. Phys. G14, 1013 (1988).

4. Y. Munehisa, Phys. Lett. **155B**, 159 (1985). G.N. Obodi, Phys. Lett. **174B**, 208 (1986). K. Farakos, G. Koutsoumbas and S. Sarantakos, National Technical University of Athens preprint, NTUA 2/88, (1988); NTUA 3/88 (1988), to appear on Zeit Phys. C. M.G. Amaral and M.E. Pol, PUC preprint 17/88, (1988); 18/88, (1988).
5. R. Pisarski, Phys. Rev. Lett. 48, 574 (1982). D. Amit and E. Rabinovici, Nucl. Phys. **B257** [FS14], 383 (1985). D.A. Kessler and H. Neuberger, Nucl. Phys. **B257**, [FS14], 695 (1985). F. Karsch and H. Meyer-Ortmanns, CERN preprint, TH.4671/87 (1987).
6. W.A. Bardeen, M. Moshe and M. Bander, Phys. Rev. Lett. 52, 1188 (1984).
7. M.G. Amaral and R.C. Shellard, PUC preprint 45/87 (1988).

### Resumo

Estudamos a estrutura de pontos tricríticos em teorias contínuas, usando a teoria  $\Phi_3^6$  em três dimensões como protótipo. Mapeamos as superfícies de transição de fase, localizando a linha tricrítica. Definimos a teoria na rede e usamos o método de Monte Carlo para fazer a simulação numérica.